The Journal of Immunology

RESEARCH ARTICLE | JULY 01 2006

# The Biological Activity of Human CD20 Monoclonal Antibodies Is Linked to Unique Epitopes on CD20[1]

Jessica L. Teeling; ... et. al

*J Immunol* (2006) 177 (1): 362–371.
https://doi.org/10.4049/jimmunol.177.1.362

# The Biological Activity of Human CD20 Monoclonal Antibodies Is Linked to Unique Epitopes on CD20[1]

**Jessica L. Teeling,[2†] Wendy J. M. Mackus,[2*] Luus J. J. M. Wiegman,* Jeroen H. N. van den Brakel,* Stephen A. Beers,[†] Ruth R. French,[†] Tom van Meerten,[‡] Saskia Ebeling,[‡] Tom Vink,* Jerry W. Slootstra,[¶] Paul W. H. I. Parren,* Martin J. Glennie,[3*†] and Jan G. J. van de Winkel*[§]**

**We have previously defined a panel of fully human CD20 mAb. Most of these were unexpectedly efficient in their ability to recruit C1q to the surface of CD20-positive cells and mediate tumor lysis via activation of the classical pathway of complement. This complement-dependent cytotoxicity (CDC) potency appeared to relate to the unusually slow off-rate of these human Abs. However, we now present epitope-mapping data, which indicates that all human mAb bind a novel region of CD20 that may influence CDC potency. Epitope mapping, using both mutagenesis studies and overlapping 15-mer peptides of the extracellular loops of CD20, defined the amino acids required for binding by an extensive panel of mouse and human mAb. Binding by rituximab and mouse CD20 mAb, had an absolute requirement for alanine and proline at positions 170 and 172, respectively, within the large extracellular loop of CD20. Surprisingly, however, all of the human CD20 mAb recognize a completely novel epitope located N-terminally of this motif, also including the small extracellular loop of CD20. Thus, although off-rate may influence biological activity of mAb, another critical factor for determining CDC potency by CD20 mAb appears to be the region of the target molecule they recognize. We conclude that recognition of the novel epitope cooperates with slow off-rate in determining the activity of CD20 Ab in activation of complement and induction of tumor cell lysis.** *The Journal of Immunology,* **2006, 177: 362–371.**

The CD20 molecule is part of the MS4A family of proteins, which are predicted to span the plasma membrane four times and contain both their C and N termini within the cell (1–3). Although the precise function of CD20 remains unknown, it appears to act as part of an ion channel expressed in the plasma membrane of both normal and malignant B cells. More specifically, Deans and colleagues (4) have recently shown that CD20 may operate as a store operated calcium ($Ca^{2+}$) channel facilitating entry of extracellular $Ca^{2+}$ following BCR-induced emptying of intracellular stores. Interestingly, despite this presumably important role, CD20-deficient mice are without obvious phenotype, which suggests that either this function is not critical for B cell physiology or that molecular redundancy exists (5). However, although questions about the biology of CD20 remain, what is irrefutable is the importance of CD20 as a target for mAb immunotherapy (3, 6–8).

The mouse/human chimeric CD20 mAb rituximab was the first cancer therapeutic mAb to be given Food and Drug Administration (FDA) approval and since then has become the most important new treatment for B cell malignancies in the last decade (9). Rituximab is now fully integrated into the management of non-Hodgkin's lymphoma patients, with most receiving mAb either as a single agent or more often given in combination with chemotherapy. It is also producing encouraging results when combined with chemotherapy in the treatment of chronic lymphocytic leukemia (CLL),[4] particularly in patients without prior therapy (10). Rituximab is furthermore finding use in autoimmune diseases, such as rheumatoid arthritis, where it has been shown to markedly improve symptoms and has recently been approved by the FDA for patients with moderate to advanced disease (11).

As a target for unconjugated mAb, CD20 appears ideal. It is highly expressed in the plasma membrane of almost all B cells, but not hematological stem cells; it normally remains at the cell surface even after cross-linking with mAb; and it is not shed from the surface to block binding by mAb (3). Although CD20 shedding has been proposed under certain conditions (12), to date this observation has not been confirmed and plasma from normal or lymphoma- or leukemia-bearing patients does not block binding of rituximab (13). Thus, collectively, these properties make CD20 an ideal target for mAb and allow efficient effector recruitment for Ab-dependent cellular cytotoxicity and complement-dependent cytotoxicity (CDC). Interestingly, in recent years, CD20 antigenic modulation has been described, particularly in CLL patients where leukemic cells become CD20 negative after rituximab treatment (14, 15). Although there have been a number of explanations of how this occurs, Taylor and colleagues (16) now suggest that the selective loss results from rituximab:CD20 complexes being stripped from the membrane of tumor cells as they pass over FcR-expressing effectors, such as Kupffer cells, a process described as CD20 shaving. However,

*Genmab, Utrecht, The Netherlands; [†]Tenovus Research Laboratory, Cancer Sciences Division, School of Medicine, University General Hospital, Southampton, United Kingdom; [‡]Department of Haematology and [§]Immunotherapy Laboratory, Department of Immunology, University Medical Center, Utrecht, The Netherlands; and [¶]Pepscan Systems BV, Lelystad, The Netherlands

Received for publication October 26, 2005. Accepted for publication March 31, 2006.

The costs of publication of this article were defrayed in part by the payment of page charges. This article must therefore be hereby marked *advertisement* in accordance with 18 U.S.C. Section 1734 solely to indicate this fact.

[1] This work was supported by Genmab and Tenovus of Cardiff.

[2] J.L.T. and W.J.M.M. are considered joint first authors.

[3] Address correspondence and reprint requests to Prof. Martin J. Glennie, Tenovus Research Laboratory, Cancer Sciences Division, School of Medicine, University General Hospital, Tremona Road, Southampton SO16 6YD, U.K. E-mail address: mjg@soton.ac.uk

[4] Abbreviations used in this paper: CLL, chronic lymphocytic leukemia; CDC, complement-dependent cytotoxicity; NHS, normal human serum; Tx-100, Triton X-100; PI, propidium iodide.



0022-1767/06/$02.00

despite occasional reports of selection of CD20-negative variants, the predominant experience with CD20 mAb, both in vitro and in vivo (17), has been that they tend not to modulate CD20 expression through internalization or down-regulation (3).

In addition to the recruitment of Ab effectors, a number of studies have shown that, when engaged by mAb, CD20 can generate transmembrane signals capable of directly controlling growth and triggering cell death in certain tumors (3, 18–22). The importance of this type of signaled cell death to the therapeutic activity of rituximab and other CD20 mAb is still not known (23). We have found that in vitro CD20 mAb differ considerably in their ability to trigger programmed cell death (3, 24). Interestingly, we find that CD20 mAb that mediate CDC effectively, such as rituximab and HuMax CD20, are relatively ineffectual, at least without extensive hyper-cross-linking, at triggering cell death directly, a property which appears to relate to their ability to translocate CD20 into lipid microdomains (25, 26). All the mAb used in the current study mediate CDC and are relatively inactive at signaling cell death. The relative importance of immune Fc-dependent effector functions and signaled cell death during lymphoma treatment is still disputed, and it seems likely that a combination of effector mechanisms underlies the therapeutic success of rituximab and other CD20 mAb (3, 9).

In the plasma membrane, CD20 is predicted to have two extracellular loops, a larger one of ~44 aa between the third and fourth transmembrane regions, and a much smaller one between the first and second transmembrane regions, which may not extend beyond the plasma membrane (27). All of the mAb described to date recognize the larger loop and partially or completely cross-block each other's binding (28, 29). Mutagenesis of the large human CD20 loop has shown that the epitopes recognized by CD20 mAb are restricted, with just two residues, alanine 170 (A170) and proline 172 (P172), being essential for binding (28). Recent work from Perosa et al. (29) has used phage displayed peptide libraries to confirm and extend these observations and show that binding by rituximab is completely dependent on P172. This narrow epitope specificity is somewhat surprising, particularly because CD20 mAb are highly diverse in their functional activity. For example, pioneering work by Clark and Tedder (30, 31) showed that two mouse IgG2a reagents, 1F5 and B1, either caused progression of resting B cells from $G_0$ into $G_1$, or blocked cell-cycle progression from $G_1$ into $G_2$/M, respectively. Similarly, although most CD20 mAb are like rituximab and promote translocation of CD20 into detergent-insoluble lipid rafts, others, such as B1 and 11B8, do not (3, 25, 32). We have shown that this property correlates with the ability to mediate CDC, because those mAb that are concentrated into lipid rafts are far more potent at recruiting C1q and activating complement. Currently, there is no explanation as to why CD20 mAb are so functionally diverse, given their restricted epitope recognition.

We previously described the performance of a panel of human CD20 mAb generated in human Ig transgenic mice. The CDC activity of these reagents was unusually potent and appeared to relate to their binding characteristics, with dissociation rate emerging as an important factor (26). In the present study, we have extended this panel to include a new human reagent, 2C6 (IgG1), which binds with a relatively fast off-rate, similar to that of rituximab, but which still displays relatively potent CDC activity, similar to the other human CD20 mAb. However, our most unexpected results come from epitope-mapping studies using mutagenesis and peptide scanning, which now show that all of the human mAb raised in the Ig transgenic mice recognize a unique region of CD20, which is located outside that seen by rituximab and a panel of mouse CD20 mAb. Recognition of this novel region together with slow off-rates appear to be two independent factors influencing the activity of CD20 Abs to induce complement activation and complement-mediated lysis.

## Materials and Methods

### *Cells and Abs*

Lymphoma cell lines were obtained from the ECACC or DZMC and cultured in supplemented RPMI 1640. HEK293F cells were obtained from Invitrogen and cultured in Freestyle medium (Invitrogen Life Technologies). Abs used in this study are listed in Table I.

### *Construction of CD20 retroviral vectors and generation of virus particles*

The CD20 cDNA was inserted into the *Bam*HI and *Not*I sites of the Moloney murine leukemia virus vector pMX under transcriptional control of the viral long terminal repeat. CD20 virus particles were produced by calcium phosphate transfection of Phoenix-ampho cells as previously described (33). Viral titers were determined by diluting virus supernatant on CEM T cells.

### *Transduction of CEM T cells and selection of CD20$^+$ clones*

In a Costar 12-well plate (Corning; Cirus), $10^5$ cells were resuspended in 2 ml of viral supernatant ($10^5$ virus particles) and culture medium in the presence of 6 $\mu$g/ml polybrene (Sigma-Aldrich). After 24 h, the infection medium was refreshed with 2 ml of culture medium. Transduction efficiency was determined after 6 days by CD20 expression on the flow cytometer. CD20$^+$ CEM cells were selected with CD20 mAb conjugated to magnetic beads according to manufacturer's instructions (Miltenyi Biotec). High (>80,000 molecules per cell) and low (<40,000 molecules per cell) CD20$^+$ cells were selected by passing the labeled cells through a magnetic cell sorting column using the sensitive positive selection program on an autoMACS cell separation device (Miltenyi Biotec). CD20$^+$ CEM clones were generated by limited dilution of the cells in 96-well plates (Nunc) at a ratio of 0.3 cells per well in 100 $\mu$l of culture medium. After 2 wk, the clones were harvested and CD20 expression was determined. Absolute

Table I. *Abs used in this study*

| Clone | Ab Isotype[a] | Supplier |
|---|---|---|
| Rituximab | Chimeric IgG1 | Roche |
| 2F2 (HuMax-CD20) | Human IgG1 | Genmab |
| 7D8 | Human IgG1 | Genmab |
| IgM 2C6 | Human IgM | Genmab |
| IgG1 2C6 | Human IgG1 class-switched from human IgM 2C6 | Genmab |
| 11B8 | Human IgG1 class-switched from human IgG3 | Genmab |
| B1 | Mouse IgG2a | Coulter |
| 2H7 | Mouse IgG2b | Serotec |
| LT20 | Mouse IgG1 | Gift from A. Filatov (Moscow, Russia) |
| 1F5 | Mouse IgG2a | ECACC hybridoma |
| AT80 | Mouse IgG1 | Tenovus |

[a] All F(ab′)$_2$ and Fab′ fragments were produced as detailed previously (44).

numbers of CD20 molecules per cell were determined using a QuantiBRITE CD20 PE kit (BD Biosciences), according to manufacturer's instructions. The mAb-bound-per-cell represents the absolute number of expressed CD20 molecules per cell. CD20 mAb conjugated with FITC was used to determine CD20 expression. WinMDI 2.8 software was used to analyze CD20 expression levels.

### *Binding of radiolabeled mAb*

mAb were trace iodinated and used in binding experiments as detailed previously (34). Briefly, $^{125}$I-labeled mAb were incubated with cells for 2 h at room temperature. Cell-bound and free $^{125}$I-labeled mAb were separated by centrifugation through a mixture of phthalate oils, allowing rapid separation without disturbing the binding equilibrium. The pelleted cells together with bound Ab were counted using a gamma counter (Wallac). mAb retained more that 90% of their binding activity following trace iodination, as measured by binding to excess CD20$^+$ cells.

### *CDC and dissociation rate of CD20 mAb*

To determine the dissociation rate and the effect on complement activation, cells were incubated with saturating FITC-labeled anti-CD20 mAb (5 $\mu$g/ml) for 1 h at 37°C. An aliquot was taken to determine the starting level of Ab binding and CDC activation. To prevent rebinding of mAb without having an effect on complement activation, we added unlabelled Fab′ fragments of rituximab at a final concentration of 300 $\mu$g/ml before incubation at 37°C. These Fab′ fragments have a binding affinity of $\sim 1.3 \times 10^{-7}$ M (26), which, although 20 times less than the parent mAb, is still sufficient to prevent rebinding of dissociated IgG when used at this concentration. Aliquots were taken over 2 h. The amount of FITC-labeled Ab remaining on the cell surface was determined by flow cytometry and expressed as a percentage of the initial binding. CDC activity was determined by adding human serum (normal human serum (NHS); 16.6% v/v or 50% v/v) to the cells followed by an additional 30-min incubation at 37°C. Propidium iodide (PI) was added and cell lysis was determined by flow cytometry as detailed previously (26).

### *Mutagenesis*

Initially, wild-type CD20 cDNA with an optimal kozak region was cloned into the expression vector pEE13.4 (Lonza), generating the vector pEE13.4CD20HS. Mutations in the extracellular regions of human CD20 were introduced using either the QuikChange XL Site-Directed Mutagenesis kit, or the QuikChange Multi Site-Directed Mutagenesis kit according to manufacturer's instructions (Stratagene). Mutagenesis was checked by restriction enzyme digestion and sequencing (AGOWA). The constructs were transiently transfected in HEK293F cells (Invitrogen Life Technologies) according to manufacturer's instructions using 293fectin (Invitrogen Life Technologies). Twenty-four hours posttransfection, these cells were used for flow cytometric binding experiments with various FITC-labeled anti-CD20 mAb. HEK293F cells were >90% viable following transfection and the flow cytometric analysis was confined to the viable cells by gating on forward scatter/side scatter.

### *CD20 peptide synthesis*

The method of using peptides to identify epitopes uses an empirical approach in which single-domain or double-domain peptides, covering the complete sequence of the two proposed extracellular regions of CD20, were synthesized in an attempt to reconstruct both linear and discontinuous epitopes for CD20 mAb. Linear 15-mer overlapping peptides were synthesized directly onto credit-card-sized polypropylene plates with the C terminus covalently coupled to the bottom of each 3-$\mu$l well (455 wells per plate), and each well containing a different peptide as described previously (35, 36).

Within each of the single-domain peptides, a cyclized dicysteine bridge was formed to insert a constrained loop in the plate-attached peptides. These cysteine-based loops were constructed using Pepscan technology (⟨www.pepscan.nl⟩). Briefly, plate-bound dicysteine containing peptides were first synthesized with cysteines spaced at between 4 and 13 aa along the peptide, for example, CXXXXC-plate, XXXCXXXXCXXXXXX-plate, or CXXXXC-plate, etc. The peptides were then cyclized by treating with a,a-dibromoxylene in aqueous solution to provide cysteine loops containing different numbers of amino acids. We find that this chemical modification provides more stable loops, than do disulfide bridges. Our experience has shown that varying the loop sizes gives the best chance of identifying complex or discontinuous epitopes. We generated 505 different single-domain looped peptides based on the 11 peptide sequences listed (LMIPAGIYAPIAVTV, KISHFLKMESLNFIR, KMESLNFIRAHTPYI, MESLNFIRAHTPYIN, YINIYNAEPANPSEK, YNAEPANPSEKNSPS, NAEPANPSEKNSPST, EPANPSEKNSPSTQY, PANPSEKNSPSTQYA, NPSEKNSPSTQYAYS, and SEKNSPSTQYAYSIQ). These peptides were partially overlapping sequences covering the complete sequences of both extracellular loops of human CD20, including the important AxP (170, 172) motif identified by Deans and colleague (28).

For the double-domain peptides, we aimed to juxtapose distant parts of the extracellular loops of CD20 in order that we might reconstruct discontinuous epitopes. Thus, using this approach, we were able to bring together distinct parts of one or both of the extracellular loops of CD20 as one peptide. A total of 400 different two-domain peptides were synthesized using empirical combinations of 20 selected 7-mer sequences in the standard format of the following: plate-XXXXXXXGXXXXXXX. The selected 20 7-mers were as follows: NFIRAHT, FIRAHTP, IRAHTPY, RAHTPYI, HFLKMES, FLKMESL, LKMESLN, KMESLNF, MESLNFI, EPANPSE, PANPSEK, ANPSEKN, NPSEKNS, PSEKNSP, SEKNSPS, EKNSPST, KNSPSTQ, NSPSTQY, PAGIAYP, and AGIYAPI, and these were selected from four regions of the CD20: HFLKMESLNFI, NFIRAHTPYI, EPANPSEKNSPSTQY, and PAGIYAPI.

### *Peptide-based ELISA*

The binding of mAb to peptides was assessed in a Pepscan-based ELISA. Each mAb was titrated to ensure that optimal binding was achieved and that nonspecific binding was avoided. Each of the credit-card-format polypropylene plates contained covalently linked peptides that were incubated overnight at 4°C with mAb, between 1 and 10 $\mu$g/ml in PBS containing 5% horse serum (v/v), 5% OVA (w/v), and 1% (v/v) Tween 80, or in an alternative blocking buffer of PBS containing 4% horse serum (v/v), and 1% (v/v) Tween 80.

After washing, the plates were incubated with a HRP-linked rabbit anti-Ab (DakoCytomation) for 1 h at 25°C. After further washing, peroxidase activity was assessed using ABTS substrate and color development quantified using a charge-coupled device camera and an image-processing system.

### *Method for epitope representation*

To analyze the Pepscan data and obtain a representation of the contribution of each of the amino acids in the CD20 sequence, we devised a novel epitope analysis method that takes all of the data obtained with the 905 peptides into account and that allows for scoring of amino acid contributions to conformational epitopes. Individual amino acids were identified by tripeptide motifs that represent the smallest unique units in the human CD20 amino acid sequence. All tripeptide motifs present in each of the 905 peptides tested were then identified and awarded the ELISA value obtained for the respective whole peptide. Next, to be able to rank the tripeptide motifs from strong to poor binding, we calculated a relative signal by dividing the ELISA value obtained for each individual motif by the average ELISA value from all 905 tested 15- to 30-mers, and sorted for decreasing value.

For each of the mAb tested, we selected all tripeptide motifs that scored >2.5. This means that the ELISA value of peptides containing these motifs was at least 2.5 times the average ELISA value of those obtained with all 905 peptides. With mAb 2C6, the scores were <2.50, and the cut-off was therefore chosen at 1.50. Finally, we deconvoluted these data into single amino acid contributions represented on the linear CD20 sequence by a scoring system. By walking along the linear CD20 sequence and by using the unique tripeptide units as a reference point, we awarded one point each time a CD20 amino acid was present in this set of high scoring peptides. The graphs in Fig. 7 show the total of points obtained for each of the single amino acids and represented for each of the mAb tested. For example, the highest scoring residue with rituximab is the P172 (~125 of the 500 high scoring tripeptide motifs contain this P).

### *Western blotting*

Raji cells were lysed on ice for 15 min in lysis buffer (20 mM Tris, 137 mM NaCl, 0.5 mM EDTA) containing protease inhibitors (1 $\mu$g/ml aprotinin, 1 $\mu$g/ml leupeptin, 1 mM $NaMoO_4$, 1 mM $NaVO_4$, 1 mM PMSF) and either 1% (v/v) Triton X-100 (Tx-100; Sigma-Aldrich) or 1% (v/v) digitonin (Sigma-Aldrich). Lysates were cleared (13,000 × *g*) and incubated overnight with appropriate Abs. Protein G-Sepharose (Amersham Biosciences) was added, and the mixture was incubated for 1 h at 4°C. The beads were washed and precipitated protein was eluted in nonreducing SDS sample buffer, separated by SDS-PAGE, and transferred to nitrocellulose (Bio-Rad). After blocking in 5% Topblock (Sigma-Aldrich) in PBS-Tween (0.5%), membranes were probed with anti-CD20 (7D1; Serotec), and bound Abs detected with HRP-conjugated rabbit anti-mouse Ab (Amersham Biosciences). Proteins were visualized using Supersignal West-Dura (Pierce) and recorded on a GeneGnome imager (Syngene).

*Statistics*

Where required, the mean ± SEM was calculated using GraphPad Prism software.

## Results

In the current work, we have continued to investigate the CDC potency of a group of human CD20 mAb. In particular, we have tested our previous hypothesis that CDC potency was directly related to binding off-rates and focused on whether the fine epitope specificity of mAb for the extracellular loops of CD20 might influence this effector function. To study the impact of CD20 expression levels on CDC by CD20 mAb in detail without the complicating factor of varying expression of complement regulatory proteins, we performed experiments with CD20-transfected human CEM T cells, which lack endogenous CD20 expression. Fig. 1 shows a panel of CD20-CEM clones expressing different amounts of CD20 varying from ~4,500 up to 135,000 molecules per cell. The human CD20 mAb 2F2 was highly effective at inducing CDC for all cell lines expressing more that 20,000 CD20 molecules per cell. In contrast, rituximab was considerably less active and never achieved full lysis even against cells expressing the highest level of CD20. Interestingly, 2F2 achieved complete lysis of any cell line expressing >60,000 molecules of CD20, and even gave appreciable lysis of cells expressing just ~4,500 CD20 molecules/cell. Rituximab did not begin to show activity until target cells were expressing at least 30,000 CD20 molecules/cell.

In our previous study (26), we observed that binding off-rate appeared to influence the complement activating potency of CD20 mAb and suggested that mAb that bound more stably might more effectively recruit C1q. To test this hypothesis further, we generated a new human mAb against CD20 called IgM 2C6, using human Ig transgenic mice (26). Briefly, HCo 7 and KM mice (Genmab) (37) were immunized with human CD20-transfected NS/0 cells and hybridomas producing human anti-CD20 mAb generated by somatic fusion methodology as described previously (26). The IgM 2C6, which was likely to have a low affinity and faster off-rate, was class switched to human IgG1 (IgG1 2C6) for comparison with the other human CD20 mAb. We then compared the binding characteristics of the switched 2C6 using a conventional saturation curve and radiolabeled $F(ab')_2$. Rituximab, 7D8 (2F2 and 7D8 show very similar activity in binding and effector function assays) and IgG1 2C6 all had similar half-maximal binding values (rituximab (0.43 μg/ml), 7D8 (0.55 μg/ml), and IgG1 2C6 (0.48 μg/ml)) and reached a similar level of saturation (Fig. 2*A*). These values are similar to those observed previously for the human CD20 mAb, including 2F2 (data not shown). We next investigated dissociation of these mAb using flow cytometry. Cells were coated with saturating FITC-labeled CD20 mAb and then 60× excess rituximab Fab′ was added as an unlabeled competitor (note: all CD20 mAb cross-compete for binding to the extracellular loop of CD20). Fig. 2*B* shows that both rituximab and IgG1 2C6 rapidly dissociated from the cells with >50% of the FITC-labeled rituximab and 70% of the IgG1 2C6 lost after just 30 min. The mAb IgG1 2C6 therefore retained the rapid dissociation characteristics expected for IgM derived V regions and behave similarly to rituximab in this experiment. In contrast, 7D8 and 2F2 (data not shown) showed minimal loss even after 2 h.

Dissociation was also confirmed functionally using the CDC assay. Duplicate samples from the surface labeling study described above were taken and fresh human serum added as a source of complement. Fig. 2*C* shows that at the start of the experiment, before adding the Fab′ competitor, all of the mAb, including IgG1

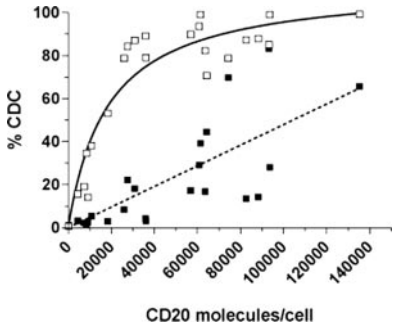


**FIGURE 1.** Anti-CD20 mediated CDC of cells expressing varying amounts of CD20. CEM cells were virally transduced with human CD20 and clones expressing different levels of CD20 selected as described in *Materials and Methods*. CDC activity was assessed by incubating each CEM-CD20 clone with 10 μg/ml 2F2 (□) or rituximab (■) mAb, adding NHS (50% v/v) as a source of complement, and determining lysis by PI exclusion in flow cytometry after 30-min incubation at 37°C. The results show that 2F2 induced significant lysis of CEM cells expressing low levels of CD20, whereas rituximab was unable to mediate full lysis of these cells, even when expressing >100,000 CD20 molecules/cell.

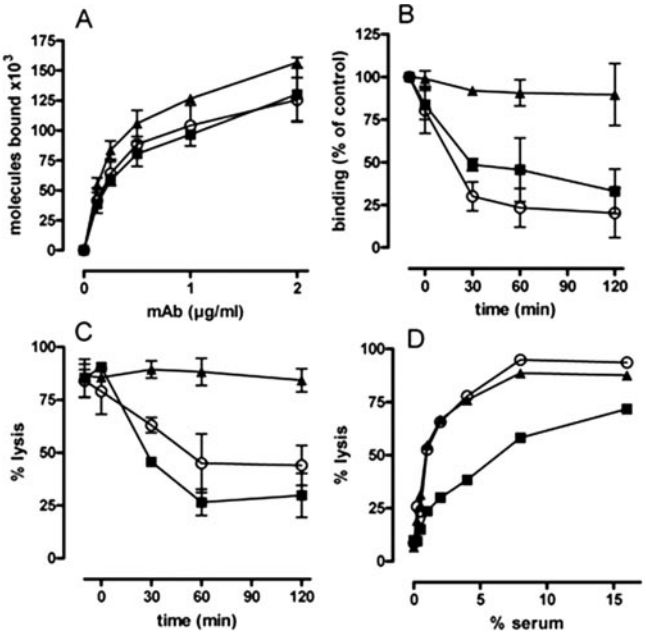


**FIGURE 2.** Binding characteristics and CDC activity of CD20 mAb. *A*, Binding curves using $^{125}$I-labeled antibodies. First, $^{125}$I-labeled IgG of rituximab (■), 7D8 (▲), and 2C6 (○) were incubated with Daudi cells for 2 h at room temperature. The cell bound and free $^{125}$I-labeled mAb were then separated by centrifugation through phthalate oils, and the cell pellets together with bound Ab were counted for radioactivity. *B* and *C*, Dissociation of CD20 mAb. Daudi cells were incubated with 5 μg/ml FITC-labeled IgG of rituximab (■), 7D8 (▲), or 2C6 (○) for 1 h at 37°C to achieve maximal binding. Excess CD20 mAb (rituximab) Fab′ fragments were then added to prevent the labeled mAb from rebinding, and at intervals over the next 2-h culture duplicate aliquots were taken to determine the levels of mAb bound to the cells (*B*) and the CDC activity of the bound mAb (*C*). The CDC activity was determined by addition of NHS (16.6% v/v) and PI exclusion as described in *Materials and Methods*. Representative of three experiments with similar results. *D*, CDC activity of CD20 mAb with increasing levels of complement (serum). Daudi cells were incubated with saturating levels (1 μg/ml) of IgG from rituximab (■), 7D8 (▲), or 2C6 (○), for 45 min at 37°C to allow binding equilibrium. Serum was then added to the level shown and after a further 30 min at 37°C, CDC was assessed by PI exclusion. This experiment was performed twice with similar results. The results in this figure are shown as mean (±SEM).

2C6 and rituximab, were able to achieve efficient lysis of Daudi cells. However, once added, the competitor caused a loss of CDC activity for both rituximab and IgG1 2C6, consistent with their fast dissociation (Fig. 2*B*). Neither 7D8 nor 2F2 (not shown) showed any appreciable loss of CDC activity during the experiment. Interestingly, although the flow cytometry showed that IgG1 2C6 dissociates somewhat faster than rituximab, over the course of these dissociation experiments it was consistently found to mediate slightly higher levels of lysis. For example, after 60 min, 50% of the rituximab and 25% of the IgG1 2C6 remained bound (Fig. 2*B*), yet in the parallel samples (Fig. 2*C*) the order of the CDC activity was reversed, with IgG1 2C6 mediating >40% lysis and rituximab close to 30% lysis. From performing this experiment three times, we found that at 60 min, the percentage lysis by IgG1 2C6 and rituximab were 52:35, 29:20, and 54:25, respectively. Thus, despite its faster off-rate, IgG1 2C6 is more efficient in CDC and requires fewer mAb molecules on the target to achieve a given amount of killing. To confirm this superior lytic activity of 2C6, we next performed CDC experiments using a saturating level of mAb (1 $\mu$g/ml) and increasing levels of complement. As shown in Fig. 2*D*, despite the relatively rapid off-rate of 2C6, it performed as well as 7D8 in this assay, whereas in contrast rituximab required at least 10 times as much serum to achieve an equivalent level of killing.

To further study the complement-activating ability of IgG1 2C6, we performed experiments with SU-DHL-4 and Raji as in our previous study. The rationale for investigating other cell lines was to test whether the superior CDC activity of 2C6 over rituximab was found when using cells that are highly sensitive (SU-DHL-4) or relatively resistant (Raji) to lysis, due to differences in the expression of CD20 and complement regulatory proteins, CD55 and CD59 (26). Fig. 3 shows that mAb 2F2, 7D8, and IgG1 2C6 were almost equal in their ability to induce lysis against the SU-DHL-4 line (Fig. 3*A*), and only against the resistant cell line, Raji, was IgG1 2C6 slightly less potent than the other human mAb (Fig. 3*B*). In contrast, rituximab had a lower titer for CDC against SU-DHL-4 cells and failed to give appreciable lysis of Raji. These data clearly show that, despite the readiness of IgG1 2C6 to dissociate (Fig. 2), its CDC activity is close to that of the other human mAb (Fig. 3), showing that fast off-rate is not synonymous with weak CDC activity.

One explanation for the disparate complement-activating activity of these Abs might relate to the way in which they recognize the extracellular loops of CD20. For example, a number of groups have suggested that CD20 can exist as a multimer consisting of at least four CD20 molecules (28, 38). Such complexes appear to be retained, at least partially, when the B cell membrane is solubilized with the detergent digitonin, but are disrupted with other detergents such as Tx-100. For example, Polyak and Deans (28) found that, although some CD20 epitopes (e.g., the mAb 2H7) were lost when Raji cells were lysed in Tx100, they were all retained with digitonin lysis. To investigate the ability of the human CD20 mAb and ritixumab to recognize CD20, we first performed immunoprecipitation followed by Western blot analysis on B cells solubilized in either digitonin or Tx-100. Fig. 4 shows that rituximab precipitated CD20 from both Tx-100 and digitonin lysates, albeit weaker in Tx-100, indicating that it binds to an epitope that remains intact under both conditions. In contrast, 2F2, 7D8, and IgG1 2C6 only precipitated CD20 from digitonin lysates, suggesting that the epitopes for the human mAb require the structural integrity of the native CD20 complex. Similar results were obtained with the other B cell lines such as SU-DHL-4 (data not shown). These data indicated that the human mAb perhaps recognized a different form of CD20 or a different epitope that is lost when the molecule is fully disrupted in Tx-100.

Previous epitope mapping studies of the extracellular loop of CD20 have indicated that alanine at position 170 (A170) and particularly proline at position 172 (P172) are critical for recognition by almost all known CD20 mAb (28, 29). Although epitope heterogeneity exists between different CD20 mAb, the A170- and P172-containing motif (A170/P172) is the common dominant feature. To examine whether A170 and P172 are also required for binding by the human CD20 mAb, we used two approaches: first, site-directed mutagenesis to generate a set of CD20 mutants, which were expressed in mammalian cells, and second, the screening of an extensive library of linear and looped peptides of human CD20 according to peptide scanning methodology.

Initial experiments confirmed the efficiency of our expression system and showed that all of the CD20 mAb recognized wild-type CD20 expressed in HEK293F cells. However, as shown in Fig. 5, mutating the A170 and the P172 to serine (the mouse equivalent for these 2 aa) completely prevented the binding of rituximab and a range of other mouse mAb against human CD20. The only mouse mAb that retained some binding was B1, which demonstrated a markedly diminished level of binding. Interestingly, even

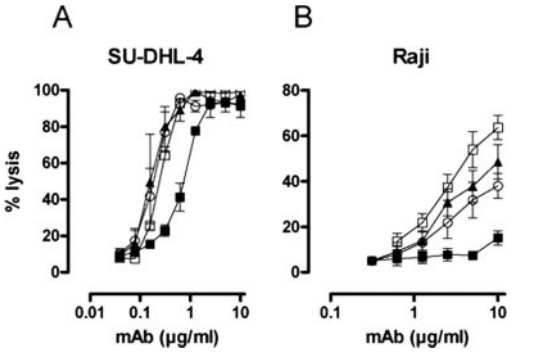


**FIGURE 3.** Anti-CD20 mAb-mediated CDC of B cell lines. SU-DHL-4 or Raji cells were incubated with different concentrations of 2F2 (□), 7D8 (▲), 2C6 (○), or rituximab (■) followed by addition of NHS (16.6% v/v) as a source of complement and incubation at 37°C for 30 min. CDC activity was determined by flow cytometry using PI exclusion as described in *Materials and Methods*. The results shown are the mean (±SEM) of at least two (SU-DHL-4) and four (Raji) separate experiments.

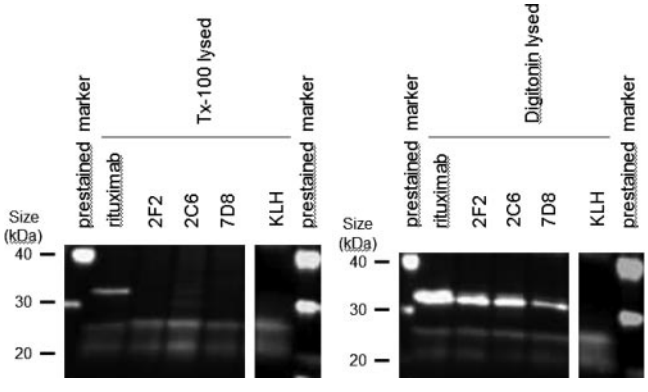


**FIGURE 4.** Differential sensitivity of CD20 epitopes to detergent lysis. Immunoprecipitation of CD20 by rituximab, 2F2, 7D8, and 2C6 from Raji B cells lysed in either 1% Tx-100 or 1% digitonin. The mAb were added to cleared (13,000 × *g*) lysates as indicated to immunoprecipitate CD20. Samples were analyzed by anti-CD20 immunoblot, as described in *Materials and Methods*. Note: the contaminating lower molecular weight bands are Ig human/chimeric L chain detected by cross-reactivity of the HRP-conjugated polyclonal rabbit anti-mouse IgG.

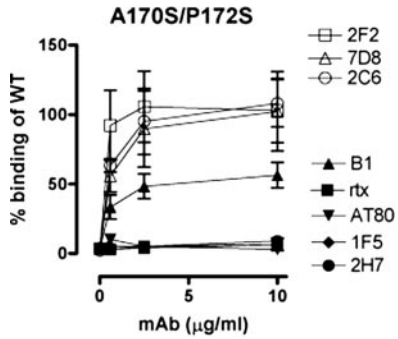


**FIGURE 5.** Ab binding to the AxP variant of the large CD20 extracellular loop. Wild-type (WT) human CD20 and the construct 2 from Table II (A170SxP172S) were expressed in HEK293F cells. Binding of the CD20 mAb was monitored by flow cytometry and the binding to construct 2 expressed as a percentage of binding to wild-type CD20. Results are expressed as the mean (±SEM) of between two and four independent experiments.

a single mutation of P172 to serine (P172S) was sufficient to totally abolish binding of these mouse mAb. These results underline the importance of the A170/P172 motif in CD20 for mouse anti-CD20 mAb binding and particularly the proline at 172. Fig. 5 also shows binding by 2F2, 7D8, and 2C6 to be unaffected by these mutations indicating that they recognize a different region of the molecule.

Human CD20 is 73% homologous to murine CD20, with most differences in the extracellular loops. To probe which amino acids were required for recognition by the human mAb, a number of amino acids were switched to the equivalent mouse residue (see Table II). The results in Fig. 6 show that changing asparagine at position 163 (N163) or asparagine at 166 (N166) into aspartic acid completely abrogated the binding of IgG1 2C6 and reduced that of 2F2 and 7D8 by up to 75%. We also generated a triple mutant with mutations at threonine 159 to lysine (T159K, N163D, and N166D). This was the only construct that failed to give binding of any of the human CD20 mAb, including 2F2 and 7D8 (Fig. 6*C*). Interestingly, mutation of T159 alone had no influence on the binding of any of the CD20 mAb tested (not shown). Finally, none of these individual mutations at T159, N163, nor N166, had any influence on the binding of rituximab or the mouse CD20 mAb. However, the triple mutant (T159K/N163D/N166D) did show a slight disruption of binding of the mouse mAb.

To confirm and extend these epitope studies, we next used Pepscan technology to generate overlapping peptides based on the sequence of the potential extracellular loops of human CD20. Pepscan is particularly suitable for epitope mapping studies, because it allows the simultaneous synthesis on solid supports of vast numbers of overlapping peptides. The immunoreactivity of multiple mAb raised against the entire protein can then be tested against these peptides. Synthetic rod-attached peptides were used to map the binding sites of a panel of mAb on the two extracellular domains of CD20 and all possible overlapping peptides in the primary sequence synthesized in steps of one amino acid. Because the epitope recognized by the human CD20 mAb appeared conformational in nature (no binding was observed to linear peptides), Pepscan was used to examine conformational epitopes. To this end, we synthesized looped peptides containing a dicysteine, which was cyclized by treating with a,a-dibromoxylene and in which the size of the loop was varied by introducing cysteine residues at variable spacing as indicated in *Materials and Methods*. To represent conformational epitopes composed of amino acids from distal points on the linear CD20, we also prepared mixed peptides. In this study, 7-mer peptides from the linear CD20 sequence were synthesized and randomly linked to each other with a single glycine residue linker. The binding of mAb to each peptide was tested in a Pepscan-based ELISA. To analyze the Pepscan data and obtain a representation of the contribution of each of the amino acids in the CD20 sequence, we devised a novel epitope analysis method that takes the data obtained with all the different peptides into account and that allows for scoring of single amino acid contributions to a conformational epitope. Fig. 7 shows the results using the extended panel of human and mouse mAb. It confirms very clearly (Fig. 7*A*) that all the mouse mAb recognize peptides centered around the A170/P172 as shown by others and confirmed in this work. Interestingly, little or no reactivity is found with peptides

Table II. *Mutations in the large extracellular loop of human CD20*[a]

| | | aa 72----------80 140----------186 |
|---|---|---|
| | Human | IPAGIYAPI NIKISHFLKMESLNFIRAHTPYINIYNCEPANPSEKNSPSTQYCYSI |
| | Mouse | IPTGVFAPI NMTLSHFLKMRRLELIQTSKPYVDIYDCEPSNSSEKNSPSTQYCNSI |
| | *Wild type* | ----------*RAHT---N--N---A-P*---------- |
| *1* | *P172S* | ----------*RAHT---N--N---A-S*---------- |
| *2* | *AxP* | ----------*RAHT---N--N---S-S*---------- |
| *3* | *N166D* | ----------*RAHT---N--D---A-P*---------- |
| *4* | *N163D* | ----------*RAHT---D--N---A-P*---------- |
| *5* | *T159K* | ----------*RAHK---N--N---A-P*---------- |
| *6* | *KDD* | ----------*RAHK---D--D---A-P*---------- |

[a] Table shows the predicted amino acid sequences for the extracellular regions (small, 72–80, and large, 140–186) of human and mouse CD20. Differences between the sequences are highlighted in gray. The proline at position 172 (bold/underlined) is critical for binding of rituximab and other mouse CD20 mAb (28, 29). The human CD20 large extracellular sequence (boxed region) was mutated to the murine sequence producing constructs 1 through 6. Mutated residues in each construct (1–6) are highlighted in gray. Wild-type human CD20 and the constructs were expressed in HEK293F cells, and binding of anti-CD20 mAb to transfected cells was monitored by flow cytometry.

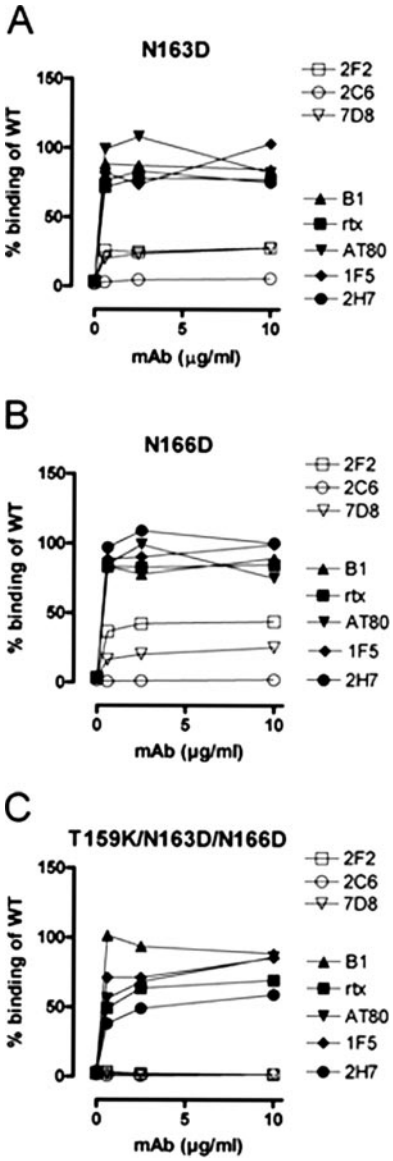


**FIGURE 6.** Ab binding to variants of the CD20 large extracellular loop. Construct 4 (N163D) (*A*), construct 3 (N166D) (*B*), and construct 6 (KDD) (*C*) from Table II and wild-type CD20 were expressed in HEK293F cells, and binding of the CD20 mAb was assessed as described in Fig. 5. Results show mean values for two to six independent experiments.

derived from the N-terminal side of A170/P172 or with the small loop of CD20, which is generally considered inaccessible to extracellular binding by mAb. In marked contrast, all three human mAb do not recognize the A170/P172-centered peptides (Fig. 7*B*) but instead bind peptides that are N-terminal of A170/P172. Finally, we also found that the three human mAb showed binding to peptides derived from the smaller of the two CD20 loops, suggesting that this is part of the exposed structure and does contribute to a CD20 epitope. This is a critical observation because it suggests that the epitopes of these human CD20 mAb might be discontinuous, i.e., contain stretches of CD20 sequence that are located on different parts of the external structure. These data are summarized in Table III and clearly underline the distinct epitope sites for the human and mouse mAb.

## Discussion

Recently, we and others have argued that one of the factors that might distinguish therapeutically effective anti-lymphoma mAb, such as rituximab and alemtuzumab, from others could be their unusual ability to activate complement, allowing lysis of tumor cells and recruitment and activation of FcR-expressing effectors (3, 15). We have now developed a range of human CD20 mAb that are surprisingly potent in CDC, one of which is in phase I/II clinical trials for the treatment of non-Hodgkin's lymphoma, B-CLL, and rheumatoid arthritis (26) (39). Their enhanced potency comes from the ability to bind and activate two to three times more C1q at the cell surface and results in lysis of fresh tumors that are resistant to CDC by rituximab (26). Target density is a critical factor for CDC, and Golay et al. (40) have shown that the success of rituximab in mediating CDC against malignant B cells is highly dependent on CD20 density. Our current results show that the human CD20 mAb are able to mediate CDC at much lower density of CD20 on the target cell surface than murine CD20 mAb. Thus, under saturating conditions, lysis with rituximab only became detectable with cells expressing ~10-fold greater numbers of CD20 molecules on their surface than it did with the human mAb, 2F2. Importantly, all of these reagents, human and rituximab, carry the same human IgG1 constant regions and capture C1q equally well when deposited on a plastic surface, thereby confirming their inherent C1q binding capacity is the same and that the marked differences seen on intact cells results from differences in mAb binding (26).

Our initial investigation pointed to the relatively slow off-rates of the human mAb to account at least partially for their CDC activity. We now tested this hypothesis by creating a rapidly dissociating human CD20 Ab by class switching the mAb IgM 2C6. This mAb, IgG1 2C6, dissociated much faster than the other human reagents and in fact even more quickly than rituximab. Surprisingly, despite this fast off-rate, IgG1 2C6 is only slightly less potent in CDC than 2F2 or 7D8 but significantly more potent than rituximab. This finding indicates that factors in addition to off-rate influence the activity of CD20 mAb in CDC. This is, furthermore, consistent with arguments that, in the in vitro assays used, complement-mediated lysis is measured in minutes, whereas the off-rate occurs over a timescale of hours.

One possible factor is the fine specificity of the human mAb. We know very little about the three-dimensional structure of CD20 or the nature of its oligomeric structure in the B cell plasma membrane. A number of workers (28, 38) have suggested that it exists as a complex of CD20 molecules, and it is also known to associate with a range of other B cell surface molecules such as CD40 and MHC class II (41, 42). We also know that its antigenic integrity relies heavily on its three-dimensional structure within the membrane. Furthermore, disrupting the membrane with detergents such as Tx-100 can result in loss of binding by CD20 mAb, again indicating that the topography of CD20 in the lipid bilayer is critical to epitope structure. Interestingly, in the current work, we found that all three of the human type I mAb (3), unlike rituximab, were unable to immunoprecipitate CD20 once the membrane had been disrupted in Tx-100. However, immunoprecipitation was successful when the membranes were solubilized in the milder detergent, digitonin. This result strongly points to a difference in the nature of the epitopes recognized by rituximab and all of the human mAb. Such results would be consistent with the human mAb requiring a discontinuous epitope provided by different parts of the larger extracellular loops, with rituximab recognizing a linear stretch, which is less sensitive to disruption.

Substitution of amino acids in the extracellular loop of human CD20 with the corresponding amino acids from mouse CD20, showed that all of the mouse anti-human CD20 mAb tested, including rituximab, were unable to bind when the alanine 170 and proline 172 were mutated to serines (A170S/P170S). This observation confirms earlier work from Polyak and Deans (28) using a

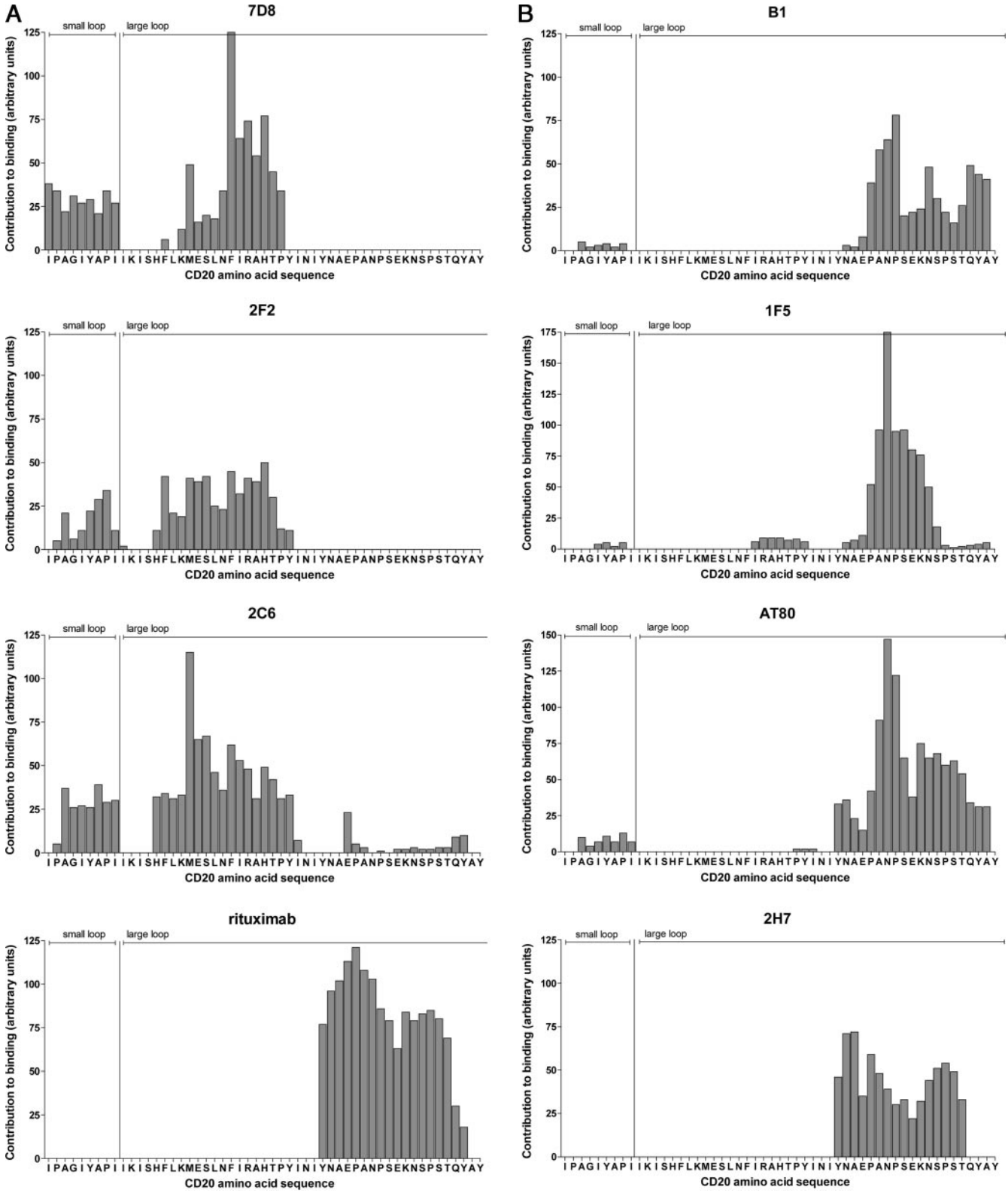


**FIGURE 7.** Analysis of the binding of human CD20 Abs to CD20 15-mer peptides. Peptides spanning the entire amino acid sequence of the extracellular loop of human CD20 were immobilized in multiwell plates and tested for their reactivity with the either human CD20 Abs (7D8, 2F2, 2C6 and rituximab) (*A*) or mouse CD20 Abs (B1, 1F5, AT80 and 2H7) (*B*). The CD20 Abs were incubated at 10 $\mu$g/ml and their binding was assessed with peroxidase-coupled rabbit anti-human IgG. The contribution of each CD20 amino acid to Ab binding (arbitrary scale) was measured as described in *Materials and Methods*.

panel of 16 mouse mAb, and the more recent results from Perosa et al. (29). Interestingly, like Perosa et al., we found that making the P170S substitution alone was sufficient to markedly reduce binding by rituximab (data not shown). This is perhaps not surprising given the tendency of prolines to introduce significant structural features into polypeptide chains, such as hairpin bends. What we did not expect, given the results with so many mouse CD20 mAb, was that such mutations would have little or no

Table III. *Pepscan epitope mapping of a panel of CD20 mAb using linear and looped peptides taken from the small and large extracellular loops of human CD20*[a]

| | *Small loop* | *----------Large loop----------* |
|---|---|---|
| 7D8 | IPAGIYAPI | NIKISHFLKMESLNFIRAHTPYINIYNCEPANPSEKNSPSTQYCY |
| 2F2 | IPAGIYAPI | NIKISHFLKMESLNFIRAHTPYINIYNCEPANPSEKNSPSTQYCY |
| 2C6 | IPAGIYAPI | NIKISHFLKMESLNFIRAHTPYINIYNCEPANPSEKNSPSTQYCY |
| RIT | IPAGIYAPI | NIKISHFLKMESLNFIRAHTPYINIYNCEPANPSEKNSPSTQYCY |
| B1 | IPAGIYAPI | NIKISHFLKMESLNFIRAHTPYINIYNCEPANPSEKNSPSTQYCY |
| 1F5 | IPAGIYAPI | NIKISHFLKMESLNFIRAHTPYINIYNCEPANPSEKNSPSTQYCY |
| AT80 | IPAGIYAPI | NIKISHFLKMESLNFIRAHTPYINIYNCEPANPSEKNSPSTQYCY |
| 2H7 | IPAGIYAPI | NIKISHFLKMESLNFIRAHTPYINIYNCEPANPSEKNSPSTQYCY |

[a] The P172, which has been found critical for the binding by rituximab, is marked in bold and underlined. Highlighted areas indicate core contact regions for the different CD20 mAb. The core amino acids were identified by testing the reactivity of CD20 mAb to a large set of linear and variable loop peptides as described in *Materials and Methods.*

influence on the binding of the human reagents. One possible explanation for this difference may relate to the type of cells used in the immunization of the human Ig mice (26). These were mouse cells expressing exogenous human CD20 and perhaps these lacked some accessory molecule(s) normally associated with human CD20, and so unmasking a new dominant epitope. Alternatively, it might relate to the use of Ig transgenic mice which express the human (as opposed to mouse) V region gene repertoire, which may favor recognition of the new epitope.

Sequential single substitutions of human for mouse amino acids along the full length of the large extracellular loop resulted in the identification of only three residues (T159K/N163D/N166D; Table II), which influenced the binding of the human mAb. Importantly, these changes had relatively little influence on the mouse mAb and thereby confirmed that human and mouse CD20 mAb recognize distinct regions of the molecule. Using Pepscan technology with multiple overlapping peptides, we were able to delineate the epitopes recognized in more detail. The analysis of a range of mouse mAb showed that they recognize a common peptide, EPANPSEK, containing the A170/P172 residues already identified (Fig. 5). This technology also confirms that the three human mAb see a distinct region FLKMESLNFIRAHTP, which is N-terminal to A170/P172. This was somewhat unexpected because the asparagines at 163 and 166, which had appeared critical in the earlier mutation study, are outside this region. The most likely explanation is that N163/N166 are important residues for maintaining the structure of the epitopes for the human mAb, even if they are not actually part of the binding site. Interestingly, the same two asparagines were suggested by Polyak and Deans (28) to influence the binding of the mouse mAb 1F5. However, in the current work and that of Perosa et al. (29), the binding of 1F5 was rituximab-like, i.e., recognized a P172-centered epitope, and was unaffected by the N163D and N166D variants.

One of the most interesting observations from this Pepscan investigation is the identification of the small loop of CD20 as a potential contact site for the human mAb. The mouse CD20 mAb, including rituximab, do not bind to this region. We have defined the small loop to contain 7 aa (AGIYAPI), and to date it has not been clear whether this loop is accessible to the extracellular space (27). However, the current work suggests that all the human mAb are making contact with this structure. Furthermore, this information, together with the immunoprecipitation data showing that CD20 binding by the human mAb was lost when membranes were disrupted in Tx-100, indicates that the human mAb recognize discontinuous epitopes, probably comprised of regions from both extracellular loops.

The current binding studies show that, despite earlier interpretations, the CDC potency of the human mAb is unlikely to be fully explained by their superior binding activity. An additional explanation may now be found in the fine specificity of these molecules. Binding to the newly identified region of CD20 could have a number of consequences that might influence CDC. It is possible that binding to this novel epitope could encourage IgG:IgG interaction which might bind C1q more efficiently, e.g., in terms of more favorable spacing or spatial projection. Solution and crystal structures of IgG show that Fc:Fc interactions can occur between Ab, with human IgG1 able to form pseudohexamers, not dissimilar in structure to IgM. This has prompted Burton and colleagues (43) to suggest that, at the target cell surface, bound Ab might participate in Fc:Fc interactions that can benefit the recruitment of effectors, such as C1q. In fact, pseudohexamers of IgG would provide a perfect structure for binding and activating C1q. Alternatively, this new epitope could be located in such a position or orientation on the CD20 complex that, when bound, the human mAb have their Fc region more proximal to the membrane. Thus, an interaction with the small 7-mer loop of CD20 might position the human CD20 mAb more closely to the membrane surface than CD20 mAb binding to the large 44-mer loop exclusively. Such close proximity of Ab Fc regions to the target membrane appears important for efficient complement lysis, probably because of the short time complement activation products remain active (26). Another possibility is that binding to the new epitope could promote more efficient translocation into lipid rafts, perhaps as a result of more efficient cross-linking of CD20 complexes. Reorganization of CD20 into these microdomains, as we have shown (3, 25), is associated with binding and activation of C1q. Although this seems a reasonable hypothesis, we have not been able to demonstrate the human mAb are any more efficient than rituximab in this respect (not shown).

This work shows for the first time that human mAb raised in Ig Tg mice recognize a unique region of the CD20 extracellular region that is not seen by other mAb. It is tempting to suggest that such epitope recognition appears closely linked with C1q capture and CDC potency. Selected reagents from this panel will make ideal clinical reagents, having favorable binding characteristics

and being minimally immunogenic in patients. One of these reagents, 2F2, which gave superior preclinical activity, is now at an advanced stage in clinical trials for follicular lymphoma and CLL and for rheumatoid arthritis. Early results are encouraging, with only the expected level of infusion-related toxicity, yet a high number of objective responses even at the lowest doses (39).

## Acknowledgments

We thank Joost Bakker for excellent work on graphics and Mark Cragg for useful discussion of these results. Gratitude is also extended to all members of the Genmab and Tenovus laboratories who provided expert technical support and valuable discussion.

## Disclosures

M. J. Glennie has a consultancy with Genmab.

## References

1. Tedder, T. F., and P. Engel. 1994. CD20: a regulator of cell-cycle progression of B lymphocytes. *Immunol. Today* 15: 450–454.
2. Liang, Y., T. R. Buckley, L. Tu, S. D. Langdon, and T. F. Tedder. 2001. Structural organization of the human MS4A gene cluster on chromosome 11q12. *Immunogenetics* 53: 357–368.
3. Cragg, M. S., C. A. Walshe, A. O. Ivanov, and M. J. Glennie. 2005. The biology of CD20 and its potential as a target for mAb therapy. *Curr. Dir. Autoimmun.* 8: 140–174.
4. Li, H., L. M. Ayer, J. Lytton, and J. P. Deans. 2003. Store-operated cation entry mediated by CD20 in membrane rafts. *J. Biol. Chem.* 278: 42427–42434.
5. O'Keefe, T. L., G. T. Williams, S. L. Davies, and M. S. Neuberger. 1998. Mice carrying a CD20 gene disruption. *Immunogenetics* 48: 125–132.
6. Coiffier, B. 2003. Monoclonal antibodies in the management of newly diagnosed, aggressive B-cell lymphoma. *Curr. Hematol. Rep.* 2: 23–29.
7. Coiffier, B. 2004. Rituximab in diffuse large B-cell lymphoma. *Clin. Adv. Hematol. Oncol.* 2: 156–157.
8. Johnson, P., and M. Glennie. 2003. The mechanisms of action of rituximab in the elimination of tumor cells. *Semin. Oncol.* 30: 3–8.
9. Glennie, M. J., and J. G. van de Winkel. 2003. Renaissance of cancer therapeutic antibodies. *Drug Discov. Today* 8: 503–510.
10. Cheson, B. D. 2006. Monoclonal antibody therapy of chronic lymphocytic leukemia. *Cancer Immunol. Immunother.* 55: 188–196.
11. Summers, K. M., and D. R. Kockler. 2005. Rituximab treatment of refractory rheumatoid arthritis. *Ann. Pharmacother.* 39: 2091–2095.
12. Manshouri, T., K. A. Do, X. Wang, F. J. Giles, S. M. O'Brien, H. Saffer, D. Thomas, I. Jilani, H. M. Kantarjian, M. J. Keating, and M. Albitar. 2003. Circulating CD20 is detectable in the plasma of patients with chronic lymphocytic leukemia and is of prognostic significance. *Blood* 101: 2507–2513.
13. Beum, P. V., A. D. Kennedy, and R. P. Taylor. 2004. Three new assays for rituximab based on its immunological activity or antigenic properties: analyses of sera and plasmas of RTX-treated patients with chronic lymphocytic leukemia and other B cell lymphomas. *J. Immunol. Methods* 289: 97–109.
14. Jilani, I., S. O'Brien, T. Manshuri, D. A. Thomas, V. A. Thomazy, M. Imam, S. Naeem, S. Verstovsek, H. Kantarjian, F. Giles, et al. 2003. Transient down-modulation of CD20 by rituximab in patients with chronic lymphocytic leukemia. *Blood* 102: 3514–3520.
15. Kennedy, A. D., P. V. Beum, M. D. Solga, D. J. DiLillo, M. A. Lindorfer, C. E. Hess, J. J. Densmore, M. E. Williams, and R. P. Taylor. 2004. Rituximab infusion promotes rapid complement depletion and acute CD20 loss in chronic lymphocytic leukemia. *J. Immunol.* 172: 3280–3288.
16. Beum, P. V., A. D. Kennedy, M. E. Williams, M. A. Lindorfer, and R. P. Taylor. 2006. The shaving reaction: Rituximab/CD20 complexes are removed from mantle cell lymphoma and chronic lymphocytic leukemia cells by THP-1 monocytes. *J. Immunol.* 176: 2600–2609.
17. Press, O. W., F. Appelbaum, J. A. Ledbetter, P. J. Martin, J. Zarling, P. Kidd, and E. D. Thomas. 1987. Monoclonal antibody 1F5 (anti-CD20) serotherapy of human B cell lymphomas. *Blood* 69: 584–591.
18. Cragg, M. S., R. R. French, and M. J. Glennie. 1999. Signaling antibodies in cancer therapy. *Curr. Opin. Immunol.* 11: 541–547.
19. Ghetie, M. A., H. Bright, and E. S. Vitetta. 2001. Homodimers but not monomers of Rituxan (chimeric anti-CD20) induce apoptosis in human B-lymphoma cells and synergize with a chemotherapeutic agent and an immunotoxin. *Blood* 97: 1392–1398.
20. Pagel, J. M., C. Laugen, L. Bonham, R. C. Hackman, D. M. Hockenbery, R. Bhatt, D. Hollenback, H. Carew, J. W. Singer, and O. W. Press. 2005. Induction of apoptosis using inhibitors of lysophosphatidic acid acyltransferase-$\beta$ and anti-CD20 monoclonal antibodies for treatment of human non-Hodgkin's lymphomas. *Clin. Cancer Res.* 11: 4857–4866.
21. Shan, D., A. K. Gopal, and O. W. Press. 2001. Synergistic effects of the fenretinide (4-HPR) and anti-CD20 monoclonal antibodies on apoptosis induction of malignant human B cells. *Clin. Cancer Res.* 7: 2490–2495.
22. Shan, D., J. A. Ledbetter, and O. W. Press. 2000. Signaling events involved in anti-CD20-induced apoptosis of malignant human B cells. *Cancer Immunol. Immunother.* 48: 673–683.
23. Byrd, J. C., S. Kitada, I. W. Flinn, J. L. Aron, M. Pearson, D. Lucas, and J. C. Reed. 2002. The mechanism of tumor cell clearance by rituximab in vivo in patients with B-cell chronic lymphocytic leukemia: evidence of caspase activation and apoptosis induction. *Blood* 99: 1038–1043.
24. Chan, H. T., D. Hughes, R. R. French, A. L. Tutt, C. A. Walshe, J. L. Teeling, M. J. Glennie, and M. S. Cragg. 2003. CD20-induced lymphoma cell death is independent of both caspases and its redistribution into Triton X-100 insoluble membrane rafts. *Cancer Res.* 63: 5480–5489.
25. Cragg, M. S., S. M. Morgan, H. T. Chan, B. P. Morgan, A. V. Filatov, P. W. Johnson, R. R. French, and M. J. Glennie. 2003. Complement-mediated lysis by anti-CD20 mAb correlates with segregation into lipid rafts. *Blood* 101: 1045–1052.
26. Teeling, J. L., R. R. French, M. S. Cragg, J. van den Brakel, M. Pluyter, H. Huang, C. Chan, P. W. Parren, C. E. Hack, M. Dechant, et al. 2004. Characterization of new human CD20 monoclonal antibodies with potent cytolytic activity against non-Hodgkin lymphomas. *Blood* 104: 1793–1800.
27. Polyak, M. J., S. H. Tailor, and J. P. Deans. 1998. Identification of a cytoplasmic region of CD20 required for its redistribution to a detergent-insoluble membrane compartment. *J. Immunol.* 161: 3242–3248.
28. Polyak, M. J., and J. P. Deans. 2002. Alanine-170 and proline-172 are critical determinants for extracellular CD20 epitopes; heterogeneity in the fine specificity of CD20 monoclonal antibodies is defined by additional requirements imposed by both amino acid sequence and quaternary structure. *Blood* 99: 3256–3262.
29. Perosa, F., E. Favoino, M. A. Caragnano, and F. Dammacco. 2005. Generation of biologically active linear and cyclic peptides has revealed a unique fine specificity of rituximab and its possible cross-reactivity with acid sphingomyelinase-like phosphodiesterase 3B precursor. *Blood* 107: 1070–1077.
30. Golay, J. T., E. A. Clark, and P. C. Beverley. 1985. The CD20 (Bp35) antigen is involved in activation of B cells from the $G_0$ to the $G_1$ phase of the cell cycle. *J. Immunol.* 135: 3795–3801.
31. Tedder, T. F., A. Forsgren, A. W. Boyd, L. M. Nadler, and S. F. Schlossman. 1986. Antibodies reactive with the B1 molecule inhibit cell cycle progression but not activation of human B lymphocytes. *Eur. J. Immunol.* 16: 881–887.
32. Deans, J. P., S. M. Robbins, M. J. Polyak, and J. A. Savage. 1998. Rapid redistribution of CD20 to a low density detergent-insoluble membrane compartment. *J. Biol. Chem.* 273: 344–348.
33. Weijtens, M., A. van Spronsen, A. Hagenbeek, E. Braakman, and A. Martens. 2002. Reduced graft-versus-host disease-inducing capacity of T cells after activation, culturing, and magnetic cell sorting selection in an allogeneic bone marrow transplantation model in rats. *Hum. Gene Ther.* 13: 187–198.
34. Tutt, A. L., R. R. French, T. M. Illidge, J. Honeychurch, H. M. McBride, C. A. Penfold, D. T. Fearon, R. M. Parkhouse, G. G. Klaus, and M. J. Glennie. 1998. Monoclonal antibody therapy of B cell lymphoma: signaling activity on tumor cells appears more important than recruitment of effectors. *J. Immunol.* 161: 3176–3185.
35. Slootstra, J. W., W. C. Puijk, G. J. Ligtvoet, J. P. Langeveld, and R. H. Meloen. 1996. Structural aspects of antibody-antigen interaction revealed through small random peptide libraries. *Mol. Divers.* 1: 87–96.
36. Timmerman, P., J. Beld, W. C. Puijk, and R. H. Meloen. 2005. Rapid and quantitative cyclization of multiple peptide loops onto synthetic scaffolds for structural mimicry of protein surfaces. *Chembiochem.* 6: 821–824.
37. Fishwild, D. M., S. L. O'Donnell, T. Bengoechea, D. V. Hudson, F. Harding, S. L. Bernhard, D. Jones, R. M. Kay, K. M. Higgins, S. R. Schramm, and N. Lonberg. 1996. High-avidity human IgG$\kappa$ monoclonal antibodies from a novel strain of minilocus transgenic mice. *Nat. Biotechnol.* 14: 845–851.
38. Bubien, J. K., L. J. Zhou, P. D. Bell, R. A. Frizzell, and T. F. Tedder. 1993. Transfection of the CD20 cell surface molecule into ectopic cell types generates a $Ca^{2+}$ conductance found constitutively in B lymphocytes. *J. Cell Biol.* 121: 1121–1132.
39. Hagenbeek, A., T. Plesner, J. Walewski, A. Hellmann, B. K. Link, and L. W. Dalby. 2004. HuMax-CD20 fully human monoclonal antibody in follicular lymphoma: first human exposure: early results of an ongoing phase I/II trial. *Blood* 104: 1400.
40. Golay, J., M. Lazzari, V. Facchinetti, S. Bernasconi, G. Borleri, T. Barbui, A. Rambaldi, and M. Introna. 2001. CD20 levels determine the in vitro susceptibility to rituximab and complement of B-cell chronic lymphocytic leukemia: further regulation by CD55 and CD59. *Blood* 98: 3383–3389.
41. Leveille, C., R. AL-Daccak, and W. Mourad. 1999. CD20 is physically and functionally coupled to MHC class II and CD40 on human B cell lines. *Eur. J. Immunol.* 29:65–74.
42. Szollosi, J., V. Horejsi, L. Bene, P. Angelisova, and S. Damjanovich. 1996. Supramolecular complexes of MHC class I, MHC class II, CD20, and tetraspan molecules (CD53, CD81, and CD82) at the surface of a B cell line JY. *J. Immunol.* 157: 2939–2946.
43. Saphire, E. O., R. L. Stanfield, M. D. Crispin, P. W. Parren, P. M. Rudd, R. A. Dwek, D. R. Burton, and I. A. Wilson. 2002. Contrasting IgG structures reveal extreme asymmetry and flexibility. *J. Mol. Biol.* 319: 9–18.
44. Glennie, M. J., H. M. McBride, A. T. Worth, and G. T. Stevenson. 1987. Preparation and performance of bispecific $F(ab'\gamma)_2$ antibody containing thioether-linked $Fab'\gamma$ fragments. *J. Immunol.* 139: 2367–2375.